Thermo-responsive antifouling study of commercial PolyCera® membranes for POME treatment

Teow Yeit Haan[*1,2], Loh Wei Chean[2] and Abdul Wahab Mohammad[1,2]

[1] *Research Centre for Sustainable Process Technology (CESPRO), Faculty of Engineering and Built Environment,*
Universiti Kebangsaan Malaysia, 43600 Bangi, Selangor, Malaysia
[2] *Department of Chemical and Process Engineering , Faculty of Engineering and Built Environment,*
Universiti Kebangsaan Malaysia, 43600 Bangi, Selangor, Malaysia

Abstract. Membrane fouling is the main drawback of membrane technology. Frequent membrane cleaning and membrane replacement are, therefore, required to reduce membrane fouling that causes permeate flux reduction, lower rejection, or higher operating pressure. Studies have proved that the alteration of membrane properties is the key controlling factor in lessening membrane fouling. Among stimuli-responsive membranes, thermo-responsive membrane is the most popular, with a drastic phase transition and swelling-shrinking behavior caused by the temperature change. In this study, the thermo-responsive ability of two commercial membranes, PolyCera® Titan membrane and PolyCera® Hydro membrane, at different temperatures was studied on the antifouling function of the membrane in palm oil mill effluent (POME) treatment. The evaluation of the membrane's thermo-responsive ability was done through three cycles of adsorption (fouling) and desorption (defouling) processes in a membrane filtration process. The experimental result depicted that PolyCera® Hydro membrane had a higher membrane permeability of 67.869 L/m^2.h.bar than PolyCera® Titan membrane at 46.011 L/m^2.h.bar. However, the high membrane permeability of PolyCera® Hydro membrane was compensated with low removal efficiency. PolyCera® Titan membrane with a smaller mean pore size had better rejection performance than PolyCera® Hydro membrane for all tested parameters. On the other hand, PolyCera® Titan membrane had a better hydrodynamic cleaning efficiency than PolyCera® Hydro membrane regardless of the hydrodynamic cleaning temperature. The best hydrodynamic cleaning performed by PolyCera® Titan membrane was at 35°C with the flux recovery ratio (FRR) of 99.17 ± 1.43%. The excellent thermo-responsive properties of the PolyCera® Titan membrane could eventually reduce the frequency of membrane replacement and lessen the use of chemicals for membrane cleaning. This outstanding exploration helps to provide a solution to the chemical industry and membrane technology bottleneck, which is the membrane fouling, thus reducing the operating cost incurred by the membrane fouling .

Keywords: fouling; thermo-responsive; PolyCera® membrane; antifouling; POME treatment

1. Introduction

The increase of palm oil demand in recent years has contributed to the rapid development of palm oil industry in Malaysia. This has directly resulted in an increase of waste produced during the palm oil processing. One of the major wastes produced from palm oil processing is palm oil mill effluent (POME), the largest source of industry wastewater in Malaysia. It is estimated that Malaysia produces around 53 million tons of POME annually (Pogaku *et al*. 2015).

POME is a colloidal suspension that contains 95%–96% water, 0.6%–0.7% oil, and 4%–5% solid. Direct discharge of POME into the water body without proper treatment could impose serious environmental problems to the ecosystem, such as the change of soil properties, air pollution, water pollution, and greenhouse gas emission, all of which attribute to the high biological oxygen demand (BOD), chemical oxygen demand (COD), oil and grease, total solids, and noxious smell (Khatun *et al*. 2017).

The commonly used commercial methods for POME treatment in Malaysia integrate anaerobic and aerobic ponding systems. However, the integrated anaerobic and aerobic ponding systems require large land area and long retention time (around 20 to 200 days), which is the main drawback of this POME treatment method (Zhang *et al*. 2008). Besides that, the treated POME through integrated anaerobic and aerobic ponding systems is unable to meet the industry's wastewater discharge standards set by relevant authority. As such, many studies have been carried out by researchers to discover alternative and efficient POME treatment method, including adsorption (Mohammed *et al*. 2014), photocatalytic process (Alhaji *et al*. 2016), biofilm reactor (Abu Bakar *et al*. 2018), microalgae treatment (Takriff *et al*. 2016), and membrane filtration (Ho *et al*. 2018). Among the aforementioned treatment methods, membrane filtration showed the most significant performance in POME treatment, with several advantages of the membrane technology, such as small footprint, consistent effluent quality, less chemical usage, as well as easy maintenance and operation .A pilot-scale integrated system that combined the sand filter and activated carbon filter as pretreatment, coupled with

---

∗Corresponding author, Senior Lecturer
  E-mail: yh_teow@ukm.edu.my

nanofiltration/reverse osmosis membrane technology, was introduced by Teow *et al.* (2016). The integrated system was able to remove large amounts of suspended solids in POME and reduce the BOD, COD, total suspended solids (TSS), total dissolved solids (TDS), color, phosphorus, turbidity, and conductivity up to 47.80%, 95.56%, 90.91%, 73.67%, 96.25%, 63.70%, 99.96%, and 73.64%, respectively (Teow *et al.* 2016).

Although the membrane technology is an effective POME treatment method in producing high quality effluent that can be potentially recycled and reused for several applications, it will encounter the membrane fouling (Sajjad *et al.* 2018). Membrane fouling is referred to the blocking of membrane pores by foulants or the adhesion of foulants on the membrane surface (Hosseini and Abdul Wahid 2015). The membrane fouling mechanism can be divided into four, namely, complete blocking, intermediate blocking, standard blocking, and a cake layer formation (Rana *et al.* 2015). Standard blocking occurs when small solutes are adsorbed into the membrane pores (Bowen *et al.* 1995). The solutes that are trapped in the membrane pores will eventually decrease the mean pore size of the membrane. In the case of complete blocking, the solutes are larger than the membrane pores. Solutes are deposited on the membrane surface, blocking the pores without superposition. In this case, the membrane resistance had increased, as the number of blocked pores increased. Intermediate blocking is somewhat similar to complete blocking. Solutes are deposited on top of the foulants are already adhered to the membrane surface. Cake layer formation occurs when the solutes are larger than the membrane pore size. The solutes settle down on the membrane surface that is already covered with solutes. Over the time, a layer of cake consisting of deposited solutes will be formed (Bowen *et al.* 1995). Frequent membrane cleaning and membrane replacement are, therefore, needed to lessen the impact of membrane fouling that caused permeate flux reduction, lower rejection, or higher operating pressure. Hence, the palm oil mills are still not implementing the membrane technology for POME treatment, as membrane cleaning through the use of chemicals might impose other environmental problems (Teow 2014).

Altering membrane properties has been recognized as the key controlling factor for membrane fouling by many researchers (Teow *et al.* 2012). Many studies have proved that the enhancement of membrane surface hydrophilicity is able to reduce the membrane fouling propensity, thus promoting higher flux recovery during the membrane filtration process (Du *et al.* 2018). However, for long-term operation, the modified hydrophilic membrane might not be effective in fouling prevention (Rana and Matsuura 2010). Therefore, membrane with stimuli-responsive properties is introduced (Zhou *et al.* 2014). Stimuli-responsive membrane can respond to the change of environmental conditions, such as temperature, pH, magnetic field, or photo/ultraviolet. Among these stimuli-responsive membranes, thermo-responsive membrane is most commonly used due to its ease of control (Wang *et al.* 2012). The polymer used for the fabrication of thermo-responsive membrane will show a drastic phase transition and swelling-shrinking behavior caused by the temperature change. In view of the physical stretches of membrane structure upon temperature swing, the thermo-responsive properties of the membrane could help to reduce the irreversible fouling, thus achieving an effective membrane cleaning by removing the foulants from the membrane surface.

In this work, the thermo-responsive ability of two commercial membranes, PolyCera® Titan membrane and PolyCera® Hydro membrane, was studied at different temperatures for the antifouling function of the membrane in POME treatment. The evaluation of membrane thermo-responsive ability was done through three cycles of adsorption (fouling) and desorption (defouling) processes in a membrane filtration process.

2. Materials and methods

2.1 Preparation of feed solution

POME is used as the feed solution for membrane performance study that was collected from aerobic-digested pond at a palm oil plantation. The collected aerobic-digested POME was preserved in cold room at a temperature below 4°C after sampling to prevent POME from undergoing biodegradation (Ghani *et al.* 2017). During the membrane filtration process, the collected aerobic-digested POME was diluted to 150 mg/L COD concentration to imitate the quality of pretreated POME (Teow *et al.* 2016). The typical characteristics of diluted aerobic-digested POME are summarized in Table 1.

2.2 Commercial PolyCera® membrane

Two types of commercially available ultrafiltration (UF) membranes are the PolyCera® Titan membrane and the PolyCera® Hydro membrane supplied by Water Planet Inc., USA, both of which were used in this study. The specifications of the membranes are summarized in Table 2.

Table 1 Typical characteristics of diluted aerobic-digested POME

Parameter	Concentration
Ammonia, NH_3-N (mg/L)	1.91
Chlorine, Cl (mg/L)	0.00
Phosphorus, PO_4^{3-} (mg/L)	2.60
TSS (mg/L)	74.00
Color (PtCo)	827.00
Hardness (Magnesium, Mg) (mg/L)	3.56
Hardness (Calcium, Ca) (mg/L)	0.00
COD (mg/L)	150.00
Conductivity (μS)	470.00
TDS (ppm)	177.00
Turbidity (NTU)	24.70

Table 2 Specifications of PolyCera® Titan membrane and PolyCera® Hydro membrane

Property	Membrane	
	PolyCera® Titan	PolyCera® Hydro
Type of filtration	UF	UF
Membrane pore size (nm)	5	10
Permeability of deionized water (LMH/bar)	250	450
Operating pH	1.0–13.5	1.0–12.0
Operating temperature (°C)	5–70	5–50
Maximum feed pressure (bar)	8.3	8.3
Maximum free chlorine tolerance (ppm)	< 1	< 2
Maximum oil and grease tolerance (mg/L)	< 500	< 5
Maximum suspended solids tolerance (mg/L)	< 200	< 200
Maximum hydrodynamic cleaning temperature (°C)	85	85
Maximum trans-membrane pressure (bar)	7.4	7.4

2.3 Membrane characterization

2.3.1 Field Emission Scanning Electron Microscope (FESEM)

The top surface morphology and cross-sectional structure of the commercial PolyCera® membranes were observed using FESEM, Zeiss MERLIN Compact (Carl Zeiss Inc., Germany). From the top surface morphology observation, the membrane samples were trimmed into small, appropriately-sized pieces, and mounted onto the sample holder using carbon tape. Whereas, from the cross-sectional structure observation, the membrane samples were soaked in liquid nitrogen, cryogenically fractured, and mounted vertically onto the sample holder. K550 sputter coater (Quorum Technologies, United Kingdom) was used to coat the outer layer of the membrane sample with a thin layer of gold under vacuum to provide electrical conductivity during FESEM analysis.

2.3.2 Atomic Force Microscope (AFM)

AFM, Park Systems NX-10 (Park Systems, South Korea) was employed to analyze the surface morphology and roughness of the membrane. Approximately 1 cm^2 membrane sample was cut and secured on top of a microscope's slide glass using a double-sided tape. The membrane surface was then scanned by a high-force flexure Z scanner in a semi-contact mode under ambient conditions. The reflected laser beam then generated a three-dimensional membrane surface topographical image. Root-mean-square roughness (R_q) value, which is the average profile height deviation from the mean line, was used to indicate the membrane surface roughness. It can be calculated from Eq. (1).

$$R_q = \sqrt{\sum_{n=1}^{N} \frac{(Zn - Z)^2}{N}} \tag{1}$$

where, N is the total number of point at the scanning area, Z_n is the distance of height from center plane at point n, and Z is the average height.

2.3.3 Membrane pore distribution

Membrane pore distribution was analyzed through gas flow/liquid displacement method with the use of capillary flow porometer, Porolux 1000 (Benelex Scientific, Belgium). Membrane sample with a diameter of 5 mm was wetted with porefil liquid (perfluoroethers). Nitrogen gas was passed through the membrane, where the gas flow was measured as a function of transmembrane pressure (TMP). The membrane pore size distribution was estimated using the PMI software (Benelex Scientific, Belgium).

2.3.4 Contact angle

Membrane surface hydrophilicity was characterized by the contact angle value on the membrane surface. The contact angle was measured using the contact angle system, EasyDropFM40Mk2 model (KRÜSS GmbH, Germany) equipped with DropShape Analysis software. Prior to the analysis, the membrane sample was stuck onto a glass slide using a double-sided tape to ensure the top surface of the membrane was facing upward and flat. A drop of deionized water (~13 μL) was then dropped onto the membrane surface using a motored microsyringe. Immediately, the image that showed the degree of angle between the water droplet, membrane surface, and air was captured by the F046B IRF high-speed camera (Stringray, Germany). The acquired image was analyzed using DropShape Analysis software. The contact angle measurement was repeated five
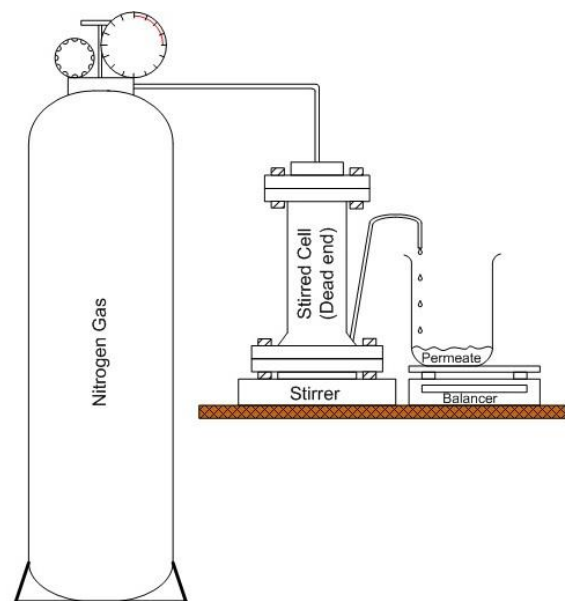

Fig. 1 Schematic diagram of a dead-end membrane filtration system

times at different spots on the membrane surface to minimize analytical error.

2.3.5 Fourier-Transform Infrared Spectroscopy (FTIR)

FTIR Nicolet 6700 (Thermo Scientific, USA) equipped with OMNI-Sampler smart accessory, coupled with a diamond crystal at an incident angle of 45°, was used to analyze the functional group that exists on the membrane surface. The FTIR spectrum was obtained from 32 scans taken at a resolution of 4 cm^{-1} and wave number ranging from 10 to 4000 cm^{-1}. The pressure applied on each membrane sample was equal to avoid differences caused by the pressure and penetrating depth.

2.3.6 Zeta potentia

The surface charge of the membrane was examined using Malvern Zetasizer Nano ZS cell (Malvern Instrument, UK). The membrane sample was cut into small coupons with a dimension of 2.5 cm × 2.5 cm. The coupon was soaked in 0.1 mM of NaCl at pH 7 for one minute. It was then stuck onto the measuring cell, with the membrane top surface facing the measuring side. The measuring cell was inserted into the cell holder of Malvern Zetasizer. Latex particles with hydrodynamic particle size ranging from 300–350 nm that were used as the tracer particle. The zeta potential was measured by Laser Doppler Electrophoresis technique. The measurement was repeated three times to minimize analytical error.

2.4 Dead-end membrane filtration system

A bench-scale dead-end membrane filtration system was used to study the performance of the membranes using diluted aerobic-digested POME as feed solution. The schematic diagram of a dead-end membrane filtration system is depicted in Fig. 1. The dead-end membrane filtration system mainly consists of a membrane dead-end stirred cell, Sterlitech HP4750 (Sterlitech Corporation, USA) with a processing volume of up to 300 mL, nitrogen gas to exert pressure on the dead-end type membrane stirred cell, pressure gauge to control and monitor the operating pressure, a stirrer to form homogeneous feed solution inside the membrane dead-end stirred cell throughout the membrane filtration process, and a balanced data acquisition system for measuring the filtrate flow.

2.5 Membrane performance study

2.5.1 Permeate flux and rejection

Flat sheet PolyCera® membrane was cut into disc shapes with a membrane effective area of 14.6 cm^2. The newly cut membrane was soaked in distilled water and left for a day to ensure the complete removal of residual solvent/chemical from the membrane. Membrane filtration was performed by laying the membrane on the membrane holder in membrane stirred cell, where it was tightened using a rubber O-ring. Permeate flux (J_v) was calculated through the direct measurement of permeate volume over time using Eq. (2). The membrane permeability was obtained from the gradient of the permeate flux against TMP in the filtration of ultrapure water.

$$J = \frac{V}{A\Delta t} \tag{2}$$

where, V is the permeate volume (m^3), A is the membrane effective area (m^2), and Δt is the operating time (h).

The effectiveness of PolyCera® membrane was assessed using diluted aerobic-digested POME as feed solution. 300 mL of diluted aerobic-digested POME was added into the membrane stirred cell. Membrane rejection was evaluated at a constant pressure of 1.5 bar and stirring speed of 400 rpm to avoid concentration polarization. Membrane rejection was calculated using Eq. (3).

$$R = \left(1 - \frac{C_p}{C_f}\right) \times 100\% \tag{3}$$

where, R is the membrane rejection (%), C_p is the concentration of the permeate (mg/L), and C_f is the concentration of the feed solution (mg/L).

2.5.2 Long-term fouling

Long-term fouling study was carried out to obtain an insight on membrane fouling behavior. Dead-end membrane filtration process was performed at a constant pressure of 1.5 bar and stirring speed of 400 rpm for 4 hours using diluted aerobic-digested POME as feed solution. Membrane fouling tendency is indicated by relative flux reduction (RFR), which calculated using Eq. (4).

$$RFR = \left(1 - \frac{J_p}{J_{p1}}\right) \times 100\% \tag{4}$$

where, J_p is the instantaneous permeate flux at specific time (L/m^2.h), and J_{p1} is the initial permeate flux (L/m^2.h).

2.5.3 Thermo-responsive antifouling

In thermo-responsive antifouling study, the dead-end membrane filtration process was performed at a constant pressure of 1.5 bar and stirring speed of 400 rpm for 10 minutes using diluted aerobic-digested POME as feed solution. Hydraulic cleaning with the use of ultrapure water was then conducted for 5 minutes at different temperatures: 25°C, 35°C, 45°C, and 50°C to determine the flux recovery of the membrane, which is correlated to the thermo-responsive antifouling ability of the membrane. Flux recovery ratio (FRR) is calculated from the water flux after hydraulic cleaning

$$FRR = \frac{J_{w2}}{J_{w1}} \times 100\% \tag{5}$$

where, J_{w1} is the initial permeate flux using distilled water as feed solution (L/m^2.h), and J_{w2} is the permeate flux of distilled water after hydraulic cleaning (L/m^2.h).

2.6 Water sample analysis

The performance of the PolyCera® membranes in

treating diluted aerobic-digested POME was evaluated by assessing the permeate water quality based on several parameters, including COD, suspended solid (SS), chlorine, NH_3-N, phosphorus, color, turbidity, and pH.

COD was measured by preheating the water sample at 150°C in Hach digital reactor DRB200 (Hach Company, USA) for 2 hours. After it was cooled to room temperature, the water sample was analyzed using DR3900 Benchtop spectrophotometer with RFID* Technology (Hach Company, USA). The SS, phosphorus, chlorine, NH_3-N, and color were measured using the photometric method, PhosVer 3 method, DPD colorimetric method, Nesslerization method, and platinum-cobalt method, respectively, using DR3900 Benchtop spectrophotometer with RFID* Technology (Hach Company, USA). Turbidity was measured by using the 2100AN turbidity meter (Hach Company, USA), whereas pH was measured by using a pH meter (Hanna Instrument, USA).

2.7 Membrane fouling model

2.7.1 Complete blocking model

Complete blocking model considers that the solutes are larger than the membrane pores, where the permeate flux is shut off by the deposition of solutes on the membrane pores. The available membrane pores will then decrease without superposition. Hence, filtrates can only pass through the unblocked pore areas. Complete blocking model is depicted by Eq. (6).

$$InJ_p = InJ_o - K_c t \tag{6}$$

where, J_p is the permeate flux (L/m^2.min), J_o is the initial permeate flux (L/m^2.min), t is the time (min), and K_c is the constant that corresponds to the complete blocking model (/min).

2.7.2 Standard blocking model

The standard blocking model accounts for fouling that occurs at the membrane's internal structure. This model considers that the solutes are smaller than the membrane pore, where the solutes can enter the membrane pore and be deposited on the pore wall. As a result, the membrane pore size decreases proportionally to the filtered permeate volume. Standard blocking model is depicted by Eq. (7).

$$\frac{1}{\sqrt{J_p}} = \frac{1}{\sqrt{J_o}} + K_s t \tag{7}$$

where, K_s is the constant that corresponds to the standard blocking model (/√m•s).

2.7.3 Intermediate blocking model

Intermediate blocking model is similar to the complete blocking model, in addition to account for the possibility that the foulants may bridge at the membrane pore entrance without completely blocking it. Intermediate blocking model is depicted by Eq. (8).

$$\frac{1}{\sqrt{J_p}} = \frac{1}{\sqrt{J_o}} + K_i t \tag{8}$$

where, K_i is the constant that corresponds to the intermediate blocking model (/m).

2.7.4 Cake layer formation model

The cake layer formation model involves large solute molecules that build up a bed of multiple solute layers over the membrane surface. The cake layer formation model is depicted by Eq. (9).

$$\frac{1}{\sqrt{J_p}^2} = \frac{1}{\sqrt{J_o}^2} + K_{gl} t \tag{9}$$

where, K_{gl} is the constant that corresponds to the cake layer formation model (s/m^2).

3. Results and discussion

3.1 Membrane characterization

Fig. 2 shows the FESEM micrographs of PolyCera® membranes' surface topology and cross-section. Comparable FESEM micrographs are observed in Fig. 2(a), where the grains are presented in both the PolyCera® Hydro membrane and the PolyCera® Titan membrane surfaces. The presence of the grains is possibly due to the silica particles incorporated into the membrane matrix during the membrane fabrication process (Zeng *et al.* 2015). On the other hand, the FESEM cross-sectional micrograph of the membrane confirms that the PolyCera® membranes are asymmetric membrane with three layers in its membrane structure—thin dense skin layer, matrix with finger-like pore structure, and spongy base layer.

The pore size distribution of PolyCera® Hydro membrane and PolyCera® Titan membrane is shown in Fig. 3. As shown in Fig. 3, both the PolyCera® Hydro membrane and the PolyCera® Titan membrane have similar membrane mean pore diameter. However, PolyCera® Hydro membrane has a narrower pore size distribution range compared to the PolyCera® Titan membrane. The narrower pore size distribution pattern shown by PolyCera® Hydro membrane indicates that this type of membrane has a more consistent membrane pore size, where the difference between the membrane pore size is insignificant. Table 3 summarizes the mean pore diameter of both the PolyCera® Hydro membrane and the PolyCera® Titan membrane. The mean pore diameter of PolyCera® Hydro membrane is 52.69 ± 2.48 nm, while the mean pore diameter of PolyCera® Titan membrane is 65.30 ± 7.00 nm. PolyCera® Hydro membrane has a smaller mean pore diameter, in which it is hypothesized to have better rejection in treating diluted aerobic-digested POME.

Fig. 4 shows the three-dimensional AFM micrographs of PolyCera® Hydro membrane and PolyCera® Titan membrane. In these AFM micrographs, the bright area represents the high point (peaks) on the membrane surface whereas the dark region indicates the low point (valleys or membrane pores) on the membrane surface. The AFM micrographs illustrated in Fig. 4 reveal that the membrane surfaces are neither smooth nor even. The PolyCera®
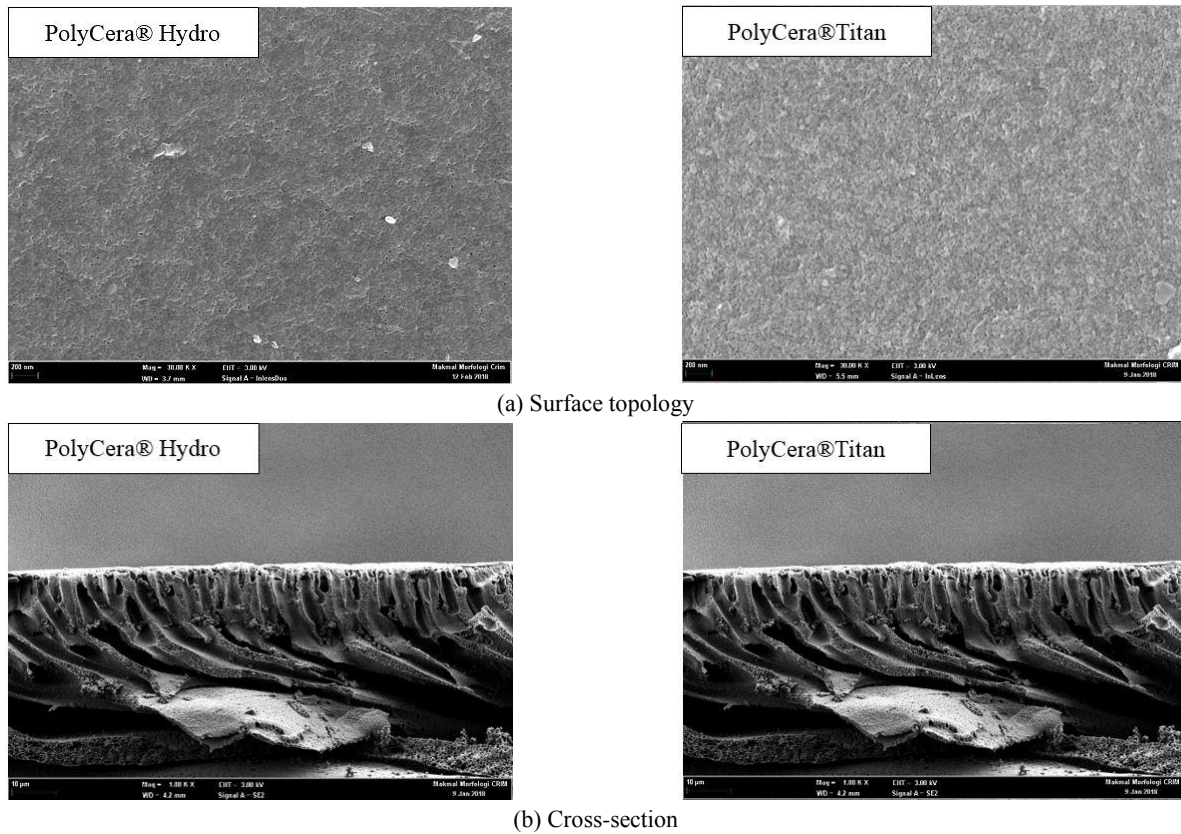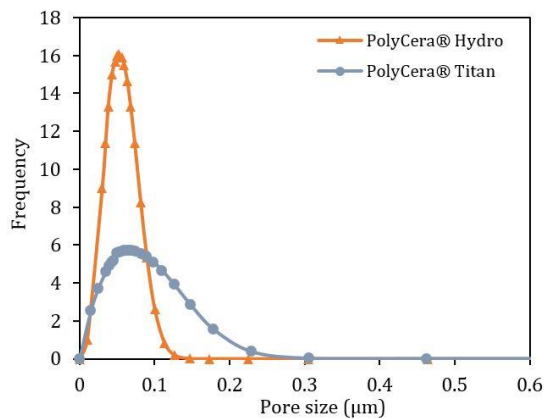
(a) Surface topology

(b) Cross-section

Fig. 2 FESEM micrographs of PolyCera® membranes

Fig. 3 Pore size distribution of PolyCera® Hydro
membrane and PolyCera® Titan membrane

Table 3 Mean pore diameter of PolyCera® Hydro
membrane and PolyCera® Titan membrane

Membrane	Mean pore diameter (nm)
PolyCera® Hydro	52.69 ± 2.48
PolyCera® Titan	65.30 ± 7.00

Hydro membrane depicted several high peaks on the membrane surface, while PolyCera® Titan membrane has a more consistent and smoother surface. The existence of high peaks on the PolyCera® Hydro membrane surface could be due to the uneven distribution of silica grains in membrane polymer during the membrane fabrication process.

The membrane surface roughness was calculated using root-mean-square roughness, R_q, which considered the ridge-and-valley structure of the membrane surface (Teow 2014). Table 4 summarizes the R_q values of the PolyCera® membranes. The higher R_q value means that more ridge-and

-valley structure was created across the membrane surface, hence, attributing to higher surface roughness. As shown in Table 4, PolyCera® Hydro membrane has a higher R_q value than PolyCera® Titan membrane. This result is consistent with the AFM micrographs in Fig. 4, whereby the PolyCera® Hydro membrane seems to have a higher surface roughness compared to PolyCera® Titan membrane. Higher surface roughness might result in an increased contact angle, as the water droplet is unable to be in direct contact with the membrane surface due to the air bubbles that are trapped in the crevasse (Ho *et al.* 2018). Therefore, PolyCera® Hydro membrane with higher surface roughness is postulated to have a higher contact angle compared to the PolyCera® Titan membrane.

The membrane surface hydrophilicity is indicated by the contact angle measurement. Generally, the lower the contact angle, the more hydrophilic the membrane surface will be. Fig. 5 shows the contact angle of PolyCera® Hydro membrane and PolyCera® Titan membrane. It is found that the contact angle of PolyCera® Titan membrane is lower than that of PolyCera® Hydro membrane. This signifies that PolyCera® Titan membrane has a higher surface

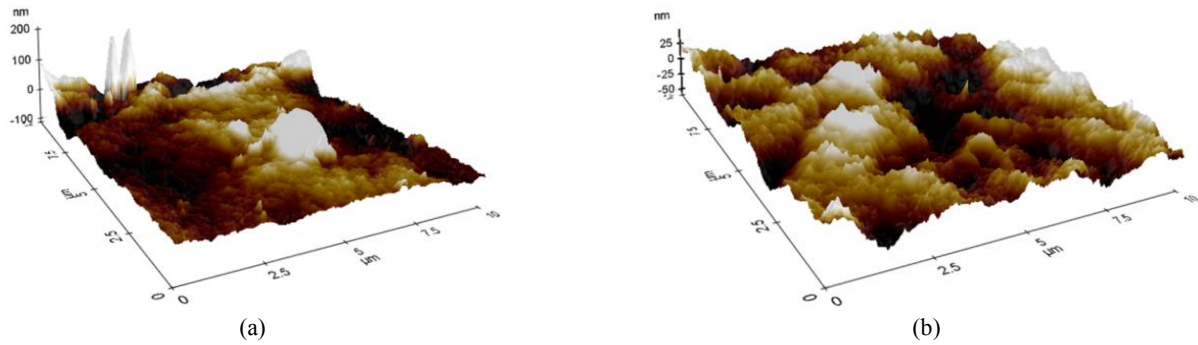(a)   (b)

Fig. 4 Three-dimensional AFM micrographs of: (a) PolyCera® Hydro membrane; and (b) PolyCera® Titan membrane

Table 4 Root-mean-square roughness of PolyCera® Hydro membrane and PolyCera® Titan membrane

Membrane	Root-mean-square roughness, R_q (nm)
PolyCera® Hydro	25.26 ± 1.78
PolyCera® Titan	14.58 ± 1.57

Fig. 5 Contact angle of PolyCera® Hydro membrane and PolyCera® Titan membrane

Fig. 6 Zeta potential of PolyCera® Hydro membrane and PolyCera® Titan membrane

a strong ability in repealing the negatively charged organic matters that exist in POME (foulants) from being adhered to the membrane surface, thus resulting in lower membrane fouling.

3.2 Membrane performance study

3.2.1 Membrane permeability

The relationship between the membrane permeate flux and the operating pressure for both PolyCera® Hydro membrane and PolyCera® Titan membrane is shown in Fig. 7. Membrane permeability is the gradient obtained from the plotted graph of membrane permeate flux against operating pressure. PolyCera® Hydro membrane has a higher membrane permeability of 67.869 L/m^2.h.bar, whereas the membrane permeability for PolyCera® Titan membrane is 46.011 L/m^2.h.bar.

Membrane permeability is mainly affected by the membrane mean pore size, surface hydrophilicity, and surface roughness. PolyCera® Titan membrane had presented a lower contact angle value (higher surface hydrophilicity) and lower surface roughness in previous surface hydrophilicity and surface roughness analyses, respectively; hence, it is expected to show a higher membrane permeability than that by the PolyCera® Hydro membrane. Conversely, an opposite observation was obtained where PolyCera® Titan membrane was having

hydrophilicity than PolyCera® Hydro membrane, which is in agreement with the postulation made from the AFM analysis. Membrane surface hydrophilicity is a significant property of the membrane. The higher surface hydrophilicity of PolyCera® Titan membrane will have a higher affinity towards water molecules, which could contribute to higher permeate flux (Teow *et al*. 2018) and lower fouling tendency that are attributed by the adsorption of hydrophobic foulants onto the membrane surface (Feng *et al*. 2012, Zhang *et al.* 2015).

The zeta potential of PolyCera® Hydro membrane and PolyCera® Titan membrane is revealed in Fig. 6. Both the PolyCera® Hydro membrane and the PolyCera® Titan membrane are negatively charged, with higher negative zeta potential value presented by the PolyCera® Hydro membrane. Zeta potential analysis provides useful information on membrane fouling. Hypothetically, most organic matters that exist in POME (foulants) are negatively charged (Ismail *et al.* 2014). Therefore, membrane with higher negative zeta potential value could demonstrate
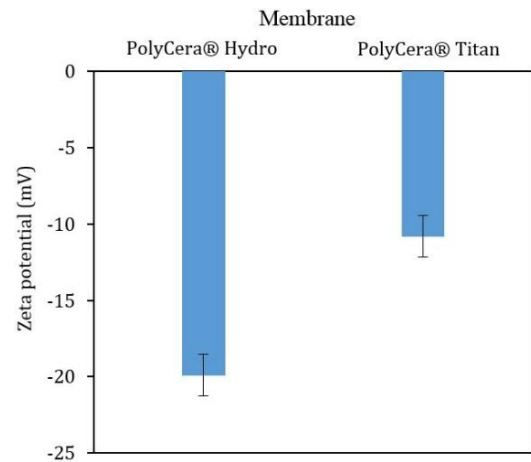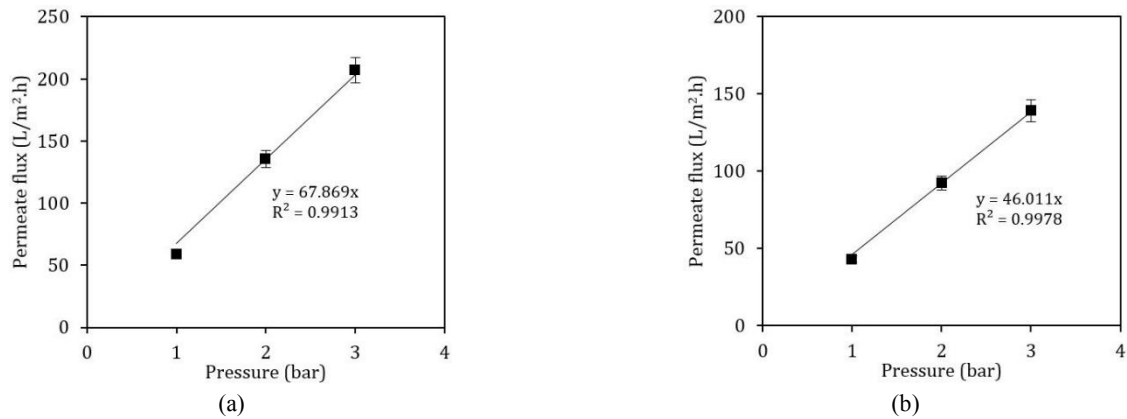
(a)　　　　　　　　　　　　　　　　　　　(b)

Fig. 7 Permeate flux and operating pressure relationship of: (a) PolyCera® Hydro membrane; and (b) PolyCera® Titan membrane

Table 5 Water quality of diluted aerobic-digested POME, treated effluent by PolyCera® Hydro membrane and PolyCera® Titan membrane; and the percent of rejection by each membrane

Parameter	Diluted aerobic-digested POME	PolyCera® Hydro		PolyCera® Titan	
		Treated effluent	Percent of rejection (%)	Treated effluent	Percent of rejection (%)
NH_3-N (mg/L)	1.91	1.42 ± 0.07	25.92	1.37 ± 0.12	28.27
COD (mg/L)	145.00	76.00 ± 2.00	47.59	34.00 ± 6.00	76.55
TSS (mg/L)	74.00	3.00 ± 0.00	95.95	2.00 ± 0.00	97.30
TDS (mg/L)	177.00	163.50 ± 2.50	7.63	161.95 ± 18.05	8.50
Color (PtCo)	827.00	153.00 ± 15.00	81.50	50.50 ± 2.50	93.89
Phosphorus (mg/L)	2.60	2.21 ± 0.26	15.00	2.06 ± 0.06	20.77
Turbidity (NTU)	24.70	0.37 ± 0.01	98.52	0.25 ± 0.01	98.98
Conductivity (µs)	470.00	326.50 ± 5.50	30.53	324.00 ± 36.00	31.06
Hardness, Mg (mg/L)	3.65	3.57 ± 0.03	2.19	3.11 ± 0.31	14.79
Hardness, Ca (mg/L)	0.00	0.00 ± 0.00	0.00	0.00 ± 0.00	0.00
Chlorine (mg/L)	0.00	0.00 ± 0.00	0.00	0.00 ± 0.00	0.00

lower membrane permeability than PolyCera® Hydro membrane. This is due to the larger mean pore size of the PolyCera® Hydro membrane (10 nm) than that of the PolyCera® Titan membrane (5 nm), as presented in Table 2. Larger mean pore size of PolyCera® Hydro membrane had allowed the water molecules to penetrate through the membrane faster and easier. Besides that, higher grain density on the PolyCera® Titan membrane surface (as shown in Fig. 2(a) FESEM micrograph) compared to PolyCera® Hydro membrane had created a denser membrane surface with higher resistance for the flow of water molecules across the membrane (Fang and Duranceau 2013). Since the membrane mean pore size and membrane structure are the dominant factors of membrane permeability, PolyCera® Titan membrane, therefore, has a lower membrane permeability than the PolyCera® Hydro membrane.

3.2.2 Membrane rejection

The water quality of aerobic-digested POME, treated effluent by PolyCera® Hydro membrane and PolyCera® Titan membrane and the percent of rejection by each membrane are summarized in Table 5. As shown in Table 5, both the PolyCera® Hydro membrane and the PolyCera® Titan membrane had demonstrated a low rejection towards phosphorus, NH_3-N, hardness, conductivity, and TDS. This is mainly attributed by the mean pore size limitation of the UF membraneA study conducted by Ho *et al.* (2017) reported that the UF membrane was unable to effectively remove the dissolved organic substances, ammonia, orthophosphates (PO_4^{3-}, HPO_4^{3-}, and $H_2PO_4^-$), and hardness ions (Ca^{2+} and Mg^{2+}). Low percent of rejection for the aforementioned parameters: phosphorus, NH_3-N, hardness, conductivity, and TDS is likely due to the electrostatic repulsion force generated between the membrane surface and the charged particles/ions.

On the other hand, both the PolyCera® Hydro membrane and the PolyCera® Titan membrane showed high removal ability towards TSS, color, and turbidity, where the percent of rejection was in the range of 95.95%–97.30%, 81.50%–93.89%, and 98.52%–98.98%, respectively. A study conducted by Said *et al.* (2015) reported that the hydrodynamic particle size of the suspended solids contained in POME was 7.5–15.0 nm.

Table 6 Comparison of water quality of treated effluent after filtering by PolyCera® Hydro membrane and PolyCera® Titan membrane with several water quality standards

Parameter	PolyCera® Hydro	PolyCera® Titan	Water quality standard			
			Boiler feed	Discharge POME	Standard A	Standard B
COD (mg/L)	76.00	34.00	< 5	-	20	50
TSS (mg/L)	3.00	2.00	< 10	400	-	-
TDS (mg/L)	163.50	161.95	< 2500	-	50	100
Color (PtCo)	153.00	50.50	-	-	100*	200*
Phosphorus (mg/L)	2.21	2.06	-	-	-	-
Turbidity (NTU)	0.37	0.25	-	-	-	-
Conductivity (µs)	326.50	324.00	-	-	-	-
pH	7.41	7.41	7–10	5–9	6–9	5.5–9

* The unit for color is ADMI
Boiler feed = Boiler feed water quality standard set by USEPA
Discharge POME = Standard F for POME discharge
Standard A/B = Malaysia's water quality standards for sewage and industry discharge

Hence, it can be separated by PolyCera® Hydro membrane and PolyCera® Titan membrane through size exclusion mechanism, as the mean pore size of the PolyCera® Hydro membrane and PolyCera® Titan membrane were 10 nm and 5 nm, respectively. Since color and turbidity parameters are directly related to the suspended solids content in diluted aerobic-digested POME (Ibrahim *et al.* 2015, Said *et al.* 2016), a high percent of TSS rejection from diluted aerobic-digested POME will also contribute to a high percent of color and turbidity rejection.

Overall, PolyCera® Titan membrane showed higher removal ability than PolyCera® Hydro membrane. Since size exclusion is a major separation mechanism for UF membrane, it is clear that PolyCera® Titan membrane with smaller mean pore size has a better rejection performance for all of the tested parameters.

In order to confirm the recyclability and reusability of the treated water, the collected permeate after it was filtered using PolyCera® Hydro membrane and PolyCera® Titan membrane was compared with several water quality standards, including the boiler feed water grade standard set by the United States Environmental Protection Agency (USEPA) for low-to-medium pressure boilers, Standard F for POME discharge, and Malaysian standard for sewage and industrial effluent discharge (Standard A and Standard B). Standard A refers to the treated water quality to be released from the upstream of water resource extraction, whereas Standard B refers to the treated water quality to be released from the downstream of water resource extraction.

Table 6 compares the water quality of the treated effluents after they were filtered using PolyCera® Hydro membrane and PolyCera® Titan membrane with several water quality standards. As presented in Table 6, the treated effluents were unable to meet the boiler feed water grade standard set by USEPA due to their high COD value (higher than 5 mg/L, as set for boiler feed water grade standard). Therefore, in order to achieve the boiler feed water grade standard for recycle and reuse purposes in palm oil mill, further treatment, such as nanofiltration or reverse osmosis membrane filtration with smaller mean pore size, is
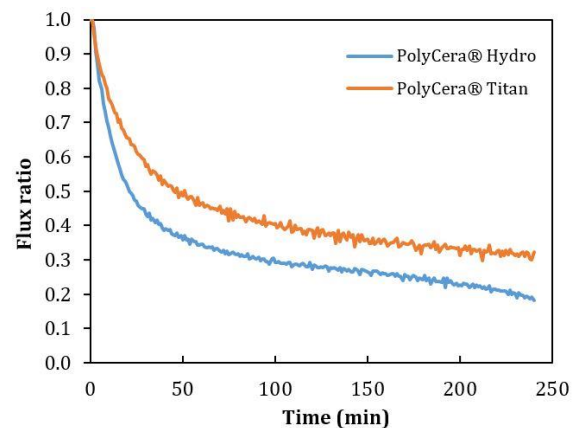

Fig. 8 Flux data of both PolyCera® Hydro membrane and PolyCera® Titan membrane for 4 hours of continuous filtration

required.

3.2.3 Membrane fouling

The flux data of both the PolyCera® Hydro membrane and PolyCera® Titan membrane for 4 hours in continuous filtration is presented in terms of their flux ratio, which is the instantaneous permeate flux over the initial permeate flux, as illustrated in Fig. 8. As shown in Fig. 8, both of the PolyCera® Hydro membrane and PolyCera® Titan membrane had experienced a sharp drop of permeate flux during the early stage of the filtration process. This indicates a drastic fouling at a fast rate due to the abundantly available membrane surface for foulants to be adsorbed onto (Teow *et al.* 2017). As the filtration process continued, the rate of permeate flux reduction had decreased proportionally with the decrease of available membrane surface for foulants' attachment. Eventually, the permeate flux approached a plateau state at the end of the filtration process, which was probably due to the formation of cake layer that had covered most of the membrane surface, thus restricting the foulants from further

accumulating onto the membrane surface.

Membrane fouling propensity is compared through the RFR value, as presented in Eq. (4). It was calculated that the RFR values for both the PolyCera® Hydro membrane and the PolyCera® Titan membrane after 4 hours of filtration process are 81.79% and 67.70%, respectively, which means that the PolyCera® Hydro membrane had a lower fouling resistance, thus experiencing a more severe membrane fouling. The calculated RFR value found was in accordance with the membrane surface roughness and surface wettability. Many researchers had reported that the membrane surface roughness is the most influential factor towards membrane fouling under the same operating conditions. PolyCera® Hydro membrane has a coarser membrane surface compared to PolyCera® Titan membrane, making it easier to trap the foulants from the feed solution (diluted aerobic-digested POME) into its valleys (membrane pores). Consequently, the foulants are adsorbed onto the membrane surface, impairing the membrane permeate flux. On the contrary, membrane fouling is also influenced by the membrane surface wettability, which is indicated by the contact angle value. As reported in the literature, hydrophilic membrane with lower contact angle value is susceptible to lower fouling propensity due to its higher affinity to water molecules, while the water shielding effect on the membrane surface prevents the hydrophobic adsorption between the foulants and the membrane surface (Zhang *et al.* 2015). Thus, PolyCera® Titan membrane with lower contact angle value (higher surface wettability) will experience lower fouling.

Permeation drag is another factor that affects membrane fouling (Ghani *et al.* 2017). High permeability of PolyCera® Hydro membrane would result in high permeation drag, which contributes to faster accumulation of the foulants onto the membrane surface. With the application of operating pressure that is perpendicular to the membrane surface in a dead-end membrane filtration system, the accumulated foulants will be forced to adhere onto the membrane surface. Apart from the membrane surface roughness, membrane surface wettability, and permeation drag, the membrane surface charge, which is indicated by the zeta potential value, also plays a role in affecting membrane fouling propensity. As reported by Said *et al.* (2015), most of the colloidal particles and natural organic matters contained in POME are negatively charged. Therefore, membranes that possess higher negative zeta potential value will demonstrate a stronger ability to repel these colloidal particles and natural organic matters from being attached to the membrane surface (Ayyaru and Ahn 2017). Surprisingly, a contradicting phenomenon was observed, where PolyCera® Hydro membrane with higher negative zeta potential value had experienced a more severe or significant fouling than PolyCera® Titan membrane. Breite *et al.* (2016) stated that the electrostatic repulsion between the membrane surface and the foulants is greatly dependent on the presence of hardness (mainly calcium and magnesium ions) in the feed solution. As shown in Table 1, there was around 3.56 mg/L of magnesium that exists in the diluted aerobic-digested POME. The presence of magnesium ions in diluted aerobic-digested POME would

Table 7 Correlation coefficient of several membrane fouling models

| Membrane | R^2 | | | |
	Standard blocking model	Complete blocking model	Intermediate blocking model	Cake layer formation model
PolyCera® Hydro	0.9823	0.9557	0.9893	0.9902
PolyCera® Titan	0.9927	0.9799	0.9943	0.9955

serve as a binding agent between the negatively charged membrane surface and the negatively charged foulants (Teow *et al.* 2017). The created electrostatic shielding effect will consequently result in a decreased electrostatic repulsion between the membrane surface and the foulants. Similar observation was obtained from a study conducted by Teow *et al.* (2017), where the electrical repulsion between the negatively charged membrane surface and the humic acid molecules was weakened by the addition of calcium ions into the feed solution. A drastic adsorption process had occurred on the membrane surface, causing a sharp drop in the permeate flux, even in the first few minutes of the membrane filtration cycle.

3.2.4 Membrane fouling model

Table 7 summarizes the R^2 of four fouling models used in this study, namely, the standard blocking model, complete blocking model, intermediate blocking model, and cake layer formation model, to explain the fouling mechanism of PolyCera® Hydro membrane and PolyCera® Titan membrane. High R^2 value for a fouling model indicates the best fit of the fouling model to the experimental data.

The R^2 value in Table 7 depicted that the declination of membrane permeate flux over filtration time for both PolyCera® Hydro membrane and PolyCera® Titan membrane in this study has a good correlation to the cake layer formation model. The cake layer is formed when the foulants have comparatively larger hydrodynamic particle size than the membrane pore size, in which only the external fouling exists. A uniform foulant layer was formed over the entire surface, this exerting resistance for the water molecules to penetrate through the membrane matrix.

3.2.5 Thermo-responsive antifouling study

The flux data that resulted from the thermo-responsive antifouling study are illustrated in Fig. 9, whereas Table 8 summarizes the calculated FRR for the PolyCera® Hydro membrane and PolyCera® Titan membrane at different cleaning temperatures. Three membrane filtration cycles were carried out for each membrane, where the hydrodynamic cleaning was conducted at different temperatures that ranged from 25°C to 55°C after each cycle of the membrane filtration process to evaluate the thermo-responsive antifouling response of both commercial membranes.
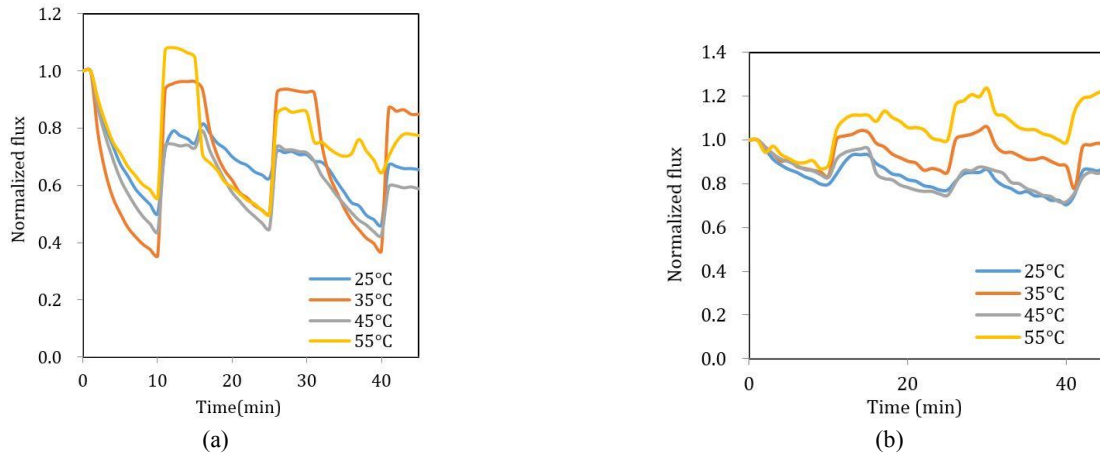
Fig. 9 Normalized flux of (a) PolyCera® Hydro membrane; and (b) PolyCera® Titan membrane in 3 consecutive membrane filtration cycles

Table 8 Flux recovery ratio of PolyCera® Hydro membrane and PolyCera® Titan at different cleaning temperature

Cleaning temperature (°C)	Flux recovery ratio, FRR (%)	
	PolyCera® Hydro	PolyCera® Titan
25	70.37 ± 4.34	89.41 ± 3.46
35	91.22 ± 5.83	99.17 ± 1.43
45	67.67 ± 7.99	89.45 ± 5.55
55	89.29 ± 13.74	119.18 ± 6.82

As presented in Fig. 9, the flux ratio for both PolyCera® Hydro membrane and PolyCera® Titan membrane had decreased as the membrane filtration process began, indicating the existence of membrane fouling. However, the flux ratio had increased significantly after undergoing the hydrodynamic cleaning process; this demonstrates the antifouling ability of the membrane. The increase in flux ratio was different in the hydrodynamic cleaning conducted at different temperatures, whereby the effectiveness of the membrane's thermo-responsive antifouling response was calculated in terms of FRR value of the membrane. Hydrodynamic cleaning temperature of the membrane with higher FRR value had higher thermo-responsive antifouling response, signifying a higher cleaning efficiency.

Table 8 shows that the permeation flux of both PolyCera® Hydro membrane and PolyCera® Titan membrane can be recovered up to 70.37%–89.41%, 91.22%–99.17%, 67.67%–89.45%, and 89.29%–119.18% for hydrodynamic cleaning at 25°C, 35°C, 45°C, and 55°C, respectively. Generally, PolyCera® Titan membrane has a better hydrodynamic cleaning efficiency (higher FRR value compared to PolyCera® Hydro membrane) regardless of the hydrodynamic cleaning temperature. Whereas, the best hydrodynamic cleaning was performed by both the PolyCera® Hydro membrane and the PolyCera® Titan membrane at 35°C. This observation indicates that the flux decline caused by diluted anaerobic POME is most likely reversible due to the reversible surface deposition. Moreover, PolyCera® Hydro membrane and PolyCera®

Titan membrane with intrinsic thermo-responsiveness or with a lower critical solution temperature (LCST) of 35°C be significantly improve the fouling propensity on the membrane surface using a hydraulic force at 35°C. When the hydrodynamic cleaning temperature is below the LCST of the membrane, the membrane will exhibit a hydrophilic property with high affinity for the penetration of water molecules across the membrane matrix. When the hydrodynamic cleaning temperature reaches the LCST of the membrane, the membrane will exhibit a hydrophobic property and becomes dehydrated. The dehydration process that occurs on the membrane matrix will result in the shrinkage of the membrane and lead to the stretching and expansion of the membrane pores. The enlargement of membrane pores enables the foulants to be flushed through the membrane. However, if the hydraulic cleaning temperature is further increased, it will not bring any significant improvement on the FRR value. On the contrary, the FRR value for PolyCera® Titan membrane at 55°C had exceeded 100%, indicating the defect on the membrane pores, where the membrane pores had grown larger than the original mean pore size of the membrane.

4. Conclusions

PolyCera® Titan membrane exhibited a lower membrane permeability than PolyCera® Hydro membrane due to the smaller mean pore size. However, since size exclusion is the major separation mechanism for UF membrane, PolyCera® Titan membrane showed a higher removal ability than PolyCera® Hydro membrane in treating diluted aerobic-digested POME, where the percent of removal for NH_3-N, COD, TSS, TDS, color, phosphorus, turbidity, conductivity, magnesium, calcium, and chlorine is 28.27%, 76.55%, 97.30%, 8.50%, 93.89%, 20.77%, 98.98%, 31.06%, 14.79%, 0.00%, and 0.00%, respectively. Nevertheless, the treated effluent after being filtered by PolyCera® Titan membrane was unable to meet the boiler feed water grade standard set by USEPA due to its high COD value. Therefore, in order to achieve the boiler feed water grade standard for recycle and reuse purposes in palm

oil mill, further treatment, such as nanofiltration or reverse osmosis membrane filtration with smaller mean pore size, is required. Additionally, PolyCera® Titan membrane has a better hydrodynamic cleaning efficiency regardless of the hydrodynamic cleaning temperature. The best hydrodynamic cleaning performed by PolyCera® Titan membrane was at a temperature of 35°C with the FRR of $99.17 \pm 1.43\%$. Therefore, PolyCera® Titan membrane with intrinsic thermo-responsiveness or with LCST at 35°C can significantly improve the fouling propensity on the membrane surface using hydraulic force at 35°C. The great thermo-responsive properties of PolyCera® Titan membrane could eventually reduce the frequency of membrane replacement and lessen the use of chemicals for membrane cleaning. This outstanding exploration helps in solving the bottleneck issue of the membrane technology, which is the membrane fouling, while reducing the operating cost incurred by membrane fouling.

Acknowledgments

References

Abu Bakar, S.N.H., Abu Hasan, H., Mohammad, A.W., Abdullah, S.R.S., Haan, T.Y., Ngteni, R. and Khairul, M.M.Y. (2018), "A review of moving-bed biofilm reactor technology for palm oil mill effluent treatment", *J. Cleaner Production*, **171**, 1532-1545. https://doi.org/10.1016/j.jclepro.2017.10.100

Ahmed, I., Balkhair, K.S., Albeiruttye, M.H. and Shaiban, A.A.J. (2018), "Importance and significance of UF/MF membrane systems in desalination water treatment", In: *Desalination*, Chapter 10, p. 187.

Alhaji, M.H., Sanaullah, K., Lim, S.F., Khan, A., Hipolito, C.N., Abdullah, M.O., Bhawani, S.A. and Jamil, T. (2016), "Photocatalytic treatment technology for palm oil mill effluent (POME) – A review", *Process Safety and Environmental Protection*, **102**, 673-686. https://doi.org/10.1016/j.psep.2016.05.020

Ayyaru, S. and Ahn, Y.-H. (2017), "Application of sulfonic acid group functionalized graphene oxide to improve hydrophilicity, permeability, and antifouling of PVDF nanocomposite ultrafiltration membranes", *J. Membr. Sci.*, **525**, 210-219. https://doi.org/10.1016/j.memsci.2016.10.048

Bowen, W.R., Calvo, J.I. and Hernández, A. (1995), "Steps of membrane blocking in flux decline during protein microfiltration", *J. Membr. Sci.*, **101**, 153-165. https://doi.org/10.1016/0376-7388(94)00295-A

Breite, D., Went, M., Prager, A. and Schulze, A. (2016), "The critical zeta potential of polymer membranes: How electrolytes impact membrane fouling", *RSC Advances*, **6**(100), 98180-98189. https://doi.org/10.1039/C6RA19239D

Du, X., Zhang, Z., Carlson, K.H., Lee, J. and Tong, T. (2018), "Membrane fouling and reusability in membrane distillation of shale oil and gas produced water: Effects of membrane surface wettability", *J. Membr. Sci.*, **567**, 199-208. https://doi.org/10.1016/j.memsci.2018.09.036

Fang, Y. and Duranceau, S.J. (2013), "Study of the effect of nanoparticles and surface morphology on reverse osmosis and nanofiltration membrane productivity", *Membranes*, **3**(3), 196-225. https://doi.org/10.3390/membranes3030196

Feng, C., Khulbe, K., Matsuura T. and Ismail, A. (2012), "Progresses in membrane and advanced oxidation processes for water treatment", *Membr. Water Treat., Int. J.*, **3**(3), 181-200. https://doi.org/10.12989/mwt.2012.3.3.181

Ghani, M.S.H., Haan, T.Y., Lun, A.W., Mohammad, A.W., Ngteni, R. and Yusof, K.M.M. (2017), "Fouling assessment of tertiary palm oil mill effluent (POME) membrane treatment for water reclamation", *J. Water Reuse Desal.*, **8**(3), 412-423. https://doi.org/10.2166/wrd.2017.198

Ho, K.C., Teow, Y.H., Ang, W.L. and Mohammad, A.W. (2017), "Novel GO/OMWCNTs mixed-matrix membrane with enhanced antifouling property for palm oil mill effluent treatment", *Separ. Purif. Technol.*, **177**, 337-349. https://doi.org/10.1016/j.seppur.2017.01.014

Ho, K.C., Teow, Y.H., Mohammad, A.W., Ang, W.L. and Lee, P.H. (2018), "Development of graphene oxide (GO)/multi-walled carbon nanotubes (MWCNTs) nanocomposite conductive membranes for electrically enhanced fouling mitigation", *J. Membr. Sci.*, **552**, 189-201. https://doi.org/10.1016/j.memsci.2018.02.001

Hosseini, S.E. and Abdul Wahid, M. (2015), "Pollutant in palm oil production process", *J. Air Waste Manag. Assoc.*, **65**(7), 773-781. https://doi.org/10.1080/10962247.2013.873092

Ibrahim, R.I., Mohammad, A.W. and Wong, Z.H. (2015), "Optimization of POME treatment process using microalgae and ultrafiltration", *Membr. Water Treat., Int. J.*, **6**(4), 293-308. https://doi.org/10.12989/mwt.2015.6.4.293

Ismail, S., Idris, I., Ng, T.Y. and Ahmad, A.L. (2014), "Coagulation of palm oil mill effluent (POME) at high temperature", *J. Appl. Sci.*, **14**(12), 1352-1254. https://doi.org/10.3923/jas.2014.1351.1354

Khatun, R., Reza, M.I.H., Moniruzzaman, M. and Yaakob, Z. (2017), "Sustainable oil palm industry: The possibilities", *Renew. Sustain. Energy Rev.*, **76**, 608-619. https://doi.org/10.1016/j.rser.2017.03.077

Mohammed, R.R., Ketabchi, M.R. and McKay, G. (2014), "Combined magnetic field and adsorption process for treatment of biologically treated palm oil mill effluent (POME)", *Chem. Eng. J.*, **243**, 31-42. https://doi.org/10.1016/j.cej.2013.12.084

Pogaku, R., Yong, K.Y. and Veera Rao, V.P.R. (2015), "Production of biogas from palm oil mill effluent", In Ravindra, P. (eds), *Adv. Bioprocess Technol.*, Springer, Cham.

Rana, D. and Matsuura, T. (2010), "Surface modifications for antifouling membranes", *Chem. Revi.*, **110**(4), 2448-2471. https://doi.org/10.1021/cr800208y

Rana, D., Matsuura, T., Kassim, M.A. and Ismail, A.F. (2015), "Reverse osmosis membrane", In: Handbook of Membrane Separations: Chemical, Pharmaceutical, Food, and Biotechnological Applications, Pabby, A.K., Rizvi, S.S.H., Sastre, A.M. (Eds.), 2nd Ed., Taylor & Francis / CRC Press, Boca Raton, FL, Chapter 3, pp. 35-52.

Said, M., Ahmad, A., Mohammad, A.W., Nor, M.T.M. and Abdullah, S.R.S. (2015), "Blocking mechanism of PES membrane during ultrafiltration of POME", *J. Industr. Eng. Chem.*, **21**, 182-188. https://doi.org/10.1016/j.jiec.2014.02.023

Said, M., Abu Hasan, H., Nor, M.T.M. and Mohammad, A.W. (2016), "Removal of COD, TSS and color from palm oil mill effluent (POME) using montmorillonite", *Desal. Water Treat.*, **57**(23), 10490-10497. https://doi.org/10.1080/19443994.2015.1036778

Sajjad, A.-A., Haan, T.Y. and Mohammad, A.W. (2018), "Sustainable approach of recycling palm oil mill effluent (POME) using integrated biofilm/membrane filtration system for internal plant usage", *Jurnal Teknologi*, **80**(4), 165-172.

https://doi.org/10.11113/jt.v80.11054

Takriff, M.S., Zakaria, M.Z., Shaiful, S.M. and Haan, T.Y. (2016), "Pre-treatments anaerobic palm oil mill effluent (POME) for microalgae treatment", *Indian J. Sci. Technol.*, **9**(12), 95248. https://doi.org/10.17485/ijst/2016/v9i21/95248

Teow, Y.H. (2014), "PVDF-TiO$_2$ mixed-matrix membrane with antifouling properties for humic acid removal", Ph.D. Dissertation; School of Chemical Engineering, Universiti Sains Malaysia, Nibong Tebal, Malaysia.

Teow, Y.H., Ooi, B.S., Ahmad, A.L. and Lim, J.K. (2012), "Mixed-matrix membrane for humic acid removal: Influence of different types of TiO$_2$ on membrane morphology and performance", *Int. J. Chem. Eng. Applicat.*, **3**(6), 374-379.

Teow Y.H., Mohammad, A.W., Hamdan, W.N.A.W.M., Ghani, M.S.H., Ngteni, R. and Yusof, K.M.M. (2016), "Pilot-scale integrated pretreatment/membrane **filtration** system for aerobic palm oil mill effluent (POME) treatment", *Proceedings of the 2016 World Congress on Advances in Civil, Environmental, and Materials Research (ACEM16)*, Jeju Island, Korea, August-September.

Teow, Y.H., Ooi, B.S. and Ahmad, A.L. (2017), "Study on PVDF-TiO$_2$ mixed-matrix membrane behavior towards humic acid adsorption", *J. Water Process Eng.*, **15**, 99-106. https://doi.org/10.1016/j.jwpe.2016.04.005

Teow, Y.H., Mubassir, S. Ho, K.C. and Mohammad, A.W. (2018), "A study on membrane technology for surface water treatment: Synthesis, characterization and performance test", *Membr. Water Treat.*, *Int. J.*, **9**(2), 69-77. https://doi.org/10.12989/mwt.2018.9.2.069

Wang, G., Xie, R., Ju, X.-J. and Chu L.-Y. (2012), "Thermo-responsive polyethersulfone composite membranes blended with poly(N-isopropylacrylamide) nanogels", *Chem. Eng. Technol.*, **35**(11), 2015-2022. https://doi.org/10.1002/ceat.201200235

Zeng, P., Wang, K., Falkenstein-Smith, R.L. and Ahn, J. (2015), "Effects of sintering temperature on the performance of SrSc$_{0.1}$Co$_{0.9}$O$_{3-\delta}$ oxygen semipermeable membrane", *Brazil. J. Chem. Eng.*, **32**(3), 757-765. https://doi.org/10.1590/0104-6632.20150323s00003269

Zhang, M., Liao, B.-q., Zhou, X., He, Y., Hong, H., Lin, H. and Chen, J. (2015), "Effects of hydrophilicity/hydrophobicity of membrane on membrane fouling in a submerged membrane bioreactor", *Bioresource Technol.*, **175**, 59-67. https://doi.org/10.1016/j.biortech.2014.10.058

Zhang, Y., Yan, L., Qiao, X., Chi, L., Niu, X., Mei, Z. and Zhang, Z. (2008), "Integration of biological method and membrane technology in treating palm oil mill effluent", *J. Environ. Sci.*, **20**(5), 558-564. https://doi.org/10.1016/S1001-0742(08)62094-X

Zhou, S., Xue, A., Zhang, Y., Li, M., Wang, J., Zhao, Y. and Xing, W. (2014), "Fabrication of temperature-responsive ZrO$_2$ tubular membranes, grafted with poly (N-isopropylacrylamide) brush chains, for protein removal and easy cleaning", *J. Membr. Sci.*, **450**, 351-361. https://doi.org/10.1016/j.memsci.2013.09.011

CC